International Journal of Computational Methods and Experimental Measurements
https://www.acadlore.com/journals/IJCMEM

Sub-Atmospheric Assisted Freshwater Tank in a Compact Multi-Effect Distillation System: Experimental Performance and Thermodynamic Evaluation

Engkos Koswara[1*], Uyung Gatot S. Dinata[2], Harun Sujadi[3], Slamet Riyadi[4], Dwi Prasetyo[1]

[1] Department of Mechanical Engineering, Universitas Majalengka, 45411 Majalengka, Indonesia
[2] Department of Mechanical Engineering, Universitas Andalas, 25163 Padang, Indonesia
[3] Department of Informatics, Universitas Majalengka, 45411 Majalengka, Indonesia
[4] Department of Mechanical Engineering, Universitas Galuh, 46251 Ciamis, Indonesia

[*] Correspondence: Engkos Koswara (ekoswara.ek@gmail.com)

Received: 10-31-2025 **Revised:** 12-13-2025 **Accepted:** 12-24-2025

Citation: E. Koswara, U. G. S. Dinata, H. Sujadi, S. Riyadi, and D. Prasetyo, "Sub-atmospheric assisted freshwater tank in a compact multi-effect distillation system: Experimental performance and thermodynamic evaluation," *Int. J. Comput. Methods Exp. Meas.*, vol. 13, no. 4, pp. 1048–1061, 2025. https://doi.org/10.56578/ijcmem130420.

© 2025 by the author(s). Licensee Acadlore Publishing Services Limited, Hong Kong. This article can be downloaded for free, and reused and quoted with a citation of the original published version, under the CC BY 4.0 license.

Abstract: The efficiency of the multi-effect distillation (MED) system is highly influenced by its operational parameters during operation. Similarly, the efficiency of the compact MED is significantly affected by its operating conditions. One of the operating parameters of MED is the pressure applied to each component. In this study, a compact MED experimental test was conducted using sub-atmospheric pressure in a freshwater tank. The freshwater tanks are designed to hold the freshwater produced by the compact MED. The installation of the freshwater tank is designed to connect to a vacuum pump to create sub-atmospheric conditions inside the freshwater tank. The highest experimental results show that under a freshwater tank pressure of 70 kPa, 368.5 mL of freshwater can be produced from 500 mL of seawater tested in a boiler at a pressure of 151.3 kPa. Based on these experimental results, sub-atmospheric pressure inside the freshwater tank can influence the output of the compact MED freshwater.

Keywords: Multi-effect distillation system; Compact multi-effect distillation; Operating parameters; Freshwater tank; Sub-atmospheric pressure

1 Introduction

Distillation is a separation technique based on the differences in boiling points or melting points of individual substances that form a homogeneous mixture [1]. In distillation, the process consists of two phases: the evaporation phase and the condensation phase, in which vapor is converted back into liquid or solid [2, 3]. Desalination of seawater is one of the most promising methods [4]. Membrane technology, particularly reverse osmosis (RO), and thermal distillation technology, including multi-stage flash (MSF) and multi-effect distillation (MED), are the two most widely used methods. The application of solar collectors in MSF systems is a step towards improving the efficiency of thermal desalination systems [5]. On the other hand, although it requires a significant amount of thermal energy, thermal distillation technology produces very high-quality water and good operational resistance at high salinity levels [6].

A simple seawater distillation dispenser (compact MED) that uses the MED method, which utilizes the heater from a typical dispenser added to the heating tube and effect tube added to the spiral pipe and nozzle as a distillation effect generator. This dispenser is capable of producing water with a lower salt content than before the distillation process [7–11].

The efficiency of a MED plant is a key factor in determining the production of freshwater, as shown by the techno-economic assessment of an MED pilot plant in Chile [12]. The annual simulations of the MED pilot plant operating with solar energy showed that the water needs can be mostly covered using a static solar thermal field with a total area of 113.2 m^2, which would generate roughly 46% of the total heat required by the water treatment plant [13]. The technical analysis has been completed with an exhaustive economic assessment, highlighting the feasibility of coupling solar fields with MED units to reduce fossil fuel dependency [14].

Heat exchangers are important for improving the distillate productivity of solar desalination systems. A heat exchanger is an essential device used for heat transfer applications, enabling efficient thermal energy utilization [15]. The present review article illustrates the application of a heat exchanger with a solar desalination system to enhance the distillate output, demonstrating that coupling these devices significantly improves freshwater yield [16]. In the current review, it is found that the heat exchanger is a critical component to improve the distillate productivity of the solar desalination system [17]. Finally, the future work and future challenges of using a heat exchanger with a solar desalination system are presented, focusing on cost reduction, scaling prevention, and long-term operational stability [18].

The distillate water collection system is an important part of seawater desalination systems, which employ various conventional and non-conventional methods [19]. Conventional and non-conventional methods are used to distil the water, and both direct and indirect collection systems are included [20]. A representative example of direct collection systems is the solar still, which utilizes solar radiation directly for evaporation and condensation [21]. Indirect collection systems, on the other hand, employ two subsystems: one for the collection of renewable energy and one for desalination, making them more adaptable to hybridization with modern energy technologies [22]. Apart from the shelter that needs to be properly designed to maintain the freshwater yield, the pressure of the freshwater tank system is very important, considering that the tank is pressurized [23]. Therefore, this research will be conducted to see the impact of the pressure of the freshwater tank. In the experiment, an experimental scheme will be carried out involving fixed variables and non-fixed variables, where the non-fixed variable will have two variables, and each variable has two levels that will be tested [24].

Recent developments in MED have concentrated on compact modular designs, vacuum-assisted processes, and improved heat recovery on the condensation side to facilitate implementation in decentralized and small-scale settings [25]. High-vacuum multiple-effect desalination systems utilizing barometric ejector-based condensation have been shown to markedly enhance vapor recovery efficiency and condensation stability [26, 27]. Pilot-scale investigations of combined MED-Absorber Compressor (MED-AB) technologies further revealed that optimizing condensation-domain thermodynamics might enhance freshwater productivity with diminished thermal input [28, 29].

Computational and parametric modelling has emerged as a significant research focus for MED development. Recent simulation-based studies highlight the optimization of pressure domains, the utilization of ejector-assisted vacuum generation, and the operation of low-temperature MED to enhance system efficiency [30, 31]. Hybrid vacuum-assisted membrane-MED (VMD-MED) systems have been suggested to improve freshwater recovery and thermal efficiency [32–34]. These investigations underscore the increasing significance of computational performance forecasting and vacuum-assisted condensation in contemporary MED design.

This study presents a compact dual-pressure-domain MED configuration, contrasting with conventional systems that operate under a uniform pressure. In this configuration, sub-atmospheric conditions are selectively applied to the freshwater recovery (condensation) domain, while the evaporation domain is independently controlled by boiler pressure. This regulated thermodynamic decoupling of vapor generation and recovery processes facilitates an increase in the condensation driving force without augmenting thermal input or system complexity, a phenomenon that has not been empirically validated in small-scale MED dispensers. This study proposes a comprehensive thermodynamic-computational evaluation framework that incorporates saturation-based pressure-temperature modelling, quantification of condensation driving forces, and effective heat transfer capacity (UA) estimation to quantitatively assess condensation-dominated freshwater recovery under sub-atmospheric conditions, thereby enabling predictive analysis of freshwater yield as a function of condensation pressure within the examined operational range.

Nevertheless, the majority of current research is on large-scale or hybrid power-plant-integrated MED systems, whereas experimental studies on small dual-pressure-domain MED systems utilizing sub-atmospheric aided freshwater recovery tanks are scarce. This study's innovation is in the experimental demonstration of a compact two-effect MED system featuring an independently regulated sub-atmospheric condensation zone, underpinned by thermodynamic-computational analysis to assess condensation-driven freshwater recovery efficacy.

2 Methodology

2.1 System Configuration and Experimental Setup

The experimental study was conducted using a compact two effect MED system specifically developed for small scale freshwater production. The system consists of a boiler chamber, two evaporation–condensation chambers (effects), a helical condenser coil, and a sub-atmospheric assisted freshwater recovery tank. A schematic representation of the experimental setup is shown in Figure 1.

The first and second effects are designed in a vertical configuration to facilitate gravity-assisted condensate flow and effective vapour-liquid interaction. Each effect is equipped with a spiral condenser, enabling thin-film evaporation and increased heat transfer area in a compact volume. The spiral condenser is made from 5/16-inch diameter copper pipe, selected for its high thermal conductivity and corrosion resistance. The fresh water recovery

tank is constructed from 4-inch diameter stainless steel pipe fitted with a pressure gauge and sub-atmospheric port. The vacuum pump is connected directly to the freshwater tank to create sub-atmospheric pressure conditions, while the evaporation chamber operates under controlled boiler pressure. This configuration allows for control of evaporation and condensation pressures in the compact MED configuration.

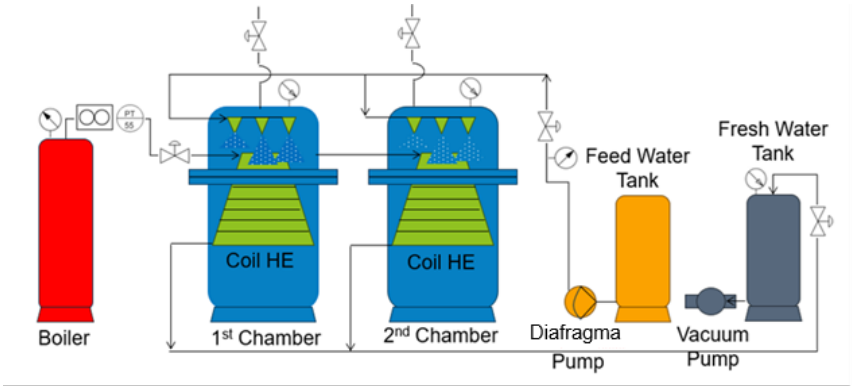

Figure 1. Schematic of the test

2.2 Operating Principles

During operation, seawater placed in the boiler chamber is heated using gas until the desired boiler pressure is reached. The steam produced by the boiler flows through the first effect, transferring latent heat and undergoing condensation in the spiral condenser. The new steam produced in the first effect enters the second effect through the spiral condenser in the second effect, where condensation occurs under sub-atmospheric pressure induced by a vacuum pump connected to a fresh water tank.

Applying sub-atmospheric pressure to freshwater tanks to lower the saturation temperature of steam during condensation. This sub-atmospheric pressure-assisted freshwater recovery mechanism aims to improve condensation efficiency and increase total freshwater production without increasing heat input or system complexity.

2.3 Experimental Variables and Test Matrix

The experimental design employed two categories of variables: fixed variables and independent (non-fixed) variables.

Fixed variables included:

- Geometry and dimensions of the first and second effect chambers.
- Length and diameter of the condenser coil.
- Seawater feed volume (500 mL per test).
- Ambient operating conditions.

Independent variables consisted of:

- Boiler pressure: 151.3 kPa and 201.3 kPa.
- Freshwater tank pressure: 80 kPa and 70 kPa.

The experimental matrix is summarized in Table 1. Each operating condition was tested individually to evaluate its influence on freshwater yield and system performance.

Table 1. Non-fixed variables

No.	Boiler Pressure (kPa)	Freshwater Tank Pressure (kPa)
1	151.3	80
2	151.3	70
3	201.3	80
4	201.3	70

2.4 Experimental Procedure

Each experimental run was conducted according to the following procedure:

- A measured volume of 500 mL of seawater was introduced into the boiler chamber.
- The condenser coil and freshwater recovery tank were connected to the system.

• The vacuum pump was activated to establish the target sub-atmospheric pressure in the freshwater tank.

• The boiler heating system was switched on, and the steam valve was gradually adjusted until the desired boiler pressure was achieved.

• Once steady-state conditions were established, freshwater condensate was collected and measured at one-minute intervals.

• Boiler pressure and freshwater tank pressure were continuously monitored to ensure stable operating conditions.

• The experiment was terminated after the predefined operating time, and the total freshwater yield was recorded.

This procedure was repeated for all combinations of boiler pressure and freshwater tank pressure listed in Table 1.

2.5 Thermodynamic and Performance Analysis Method

Thermodynamic analysis methods are used to evaluate freshwater production, condensation behaviour, and thermal performance of compact MED systems operating under freshwater recovery conditions with the aid of sub-atmospheric pressure.

This analytical approach combines thermodynamic analysis and condensation rate. Figure 2 shows the scheme used in the computational method using Aspen Hysys to predict fresh water production.

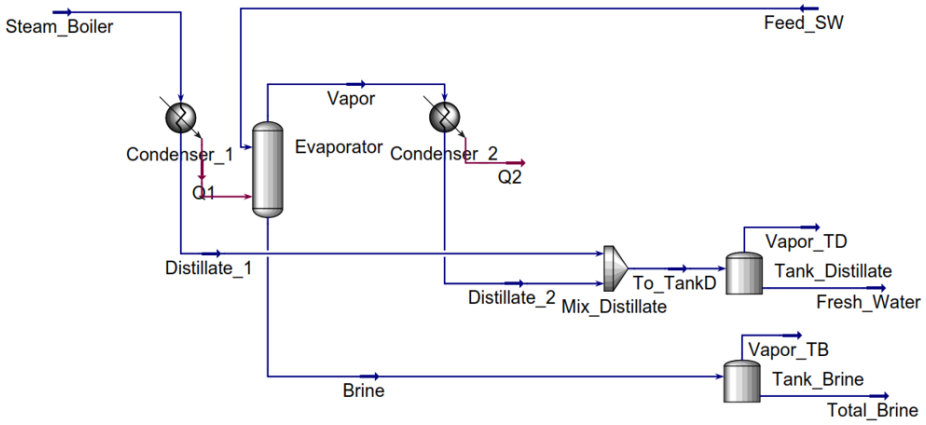

Figure 2. Flowsheet Aspen Hysys compact multi-effect distillation (MED)

2.5.1 Saturation pressure–temperature relationship

This study utilises the Clausius-Clapeyron equation, which is an equilibrium thermodynamic approach that assumes optimal phase change behaviour between the saturated liquid phase and the saturated vapour phase. In compact MED operations, experimental testing is limited in terms of conditioning the state level in each effect. Such conditions can cause deviations from optimal conditions, especially during the condensation process with the aid of sub-atmospheric pressure. Therefore, the Clausius-Clapeyron equation is used here as a primary thermodynamic indicator to describe variations in saturation temperature and condensation driving force trends, rather than as an accurate representation of conditions in the experiment.

The saturation temperature corresponding to the operating pressure in the boiler and fresh water tank is determined to define the evaporation and condensation limits of the system. The pressure-temperature relationship of saturated water vapor is approximated using the Clausius-Clapeyron equation:

$$\ln\left(\frac{P_2}{P_1}\right) = -\frac{\Delta H_{\text{vap},m}}{R}\left(\frac{1}{T_2} - \frac{1}{T_1}\right) \tag{1}$$

where,

P is the absolute pressure (Pa),

T is the saturation temperature (K),

$\Delta H_{\text{vap},m}$ is the molar latent heat of vaporization (J·mol^{-1}),

R is the universal gas constant (8.314 J·mol^{-1}·K^{-1}).

This formulation enables estimation of the saturation temperature at sub-atmospheric freshwater tank pressures, which governs condensation behaviour under sub-atmospheric assisted conditions.

2.5.2 Condensation driving force evaluation

The effective thermal driving force for condensation was evaluated using the temperature difference between saturated vapor at the boiler pressure and saturated condensate at the freshwater tank pressure:

$$\Delta T_{\text{cond}} = T_{\text{sat,boiler}} - T_{\text{sat,fw}} \tag{2}$$

This parameter provides a first-order indication of condensation intensity. Lower freshwater tank pressures reduce $T_{\text{sat,fw}}$, thereby increasing ΔT_{cond} and promoting enhanced condensation under sub-atmospheric assisted conditions.

2.5.3 Condensation heat duty and vapor utilization

The minimum heat transfer rate associated with condensation was estimated from the measured freshwater production using:

$$\dot{Q}_{\text{cond}} = \dot{m}_{fw} \cdot h_{fg} \tag{3}$$

where,

$\dot{Q}_{\text{cond}}$ is the condensation heat duty (W),

$\dot{m}_{fw}$ is the freshwater mass flow rate (kg·s^{-1}),

h_{fg} is the latent heat of vaporization (J·kg^{-1}).

This formulation links experimentally measured freshwater yield directly to thermal energy transfer, enabling a quantitative comparison of thermal performance across different pressure configurations.

2.5.4 Effective heat transfer capacity estimation

The effective UA was assessed by correlating the experimentally determined freshwater production with the condensation heat duty and the overall temperature gradient across the condenser. For each experimental run, the condensation heat duty was initially calculated from the measured freshwater mass flow rate utilizing Eq. (3). The entire heat transfer capacity was subsequently determined by:

$$UA = \frac{\dot{Q}_{\text{cond}}}{\Delta T_{\text{cond}}} \tag{4}$$

where, ΔT_{lm} is the logarithmic mean temperature difference between the saturation temperature of vapor entering the condenser (at boiler pressure) and the saturation temperature corresponding to the freshwater tank pressure. Since condensation occurs under nearly isothermal conditions, ΔT_{lm} was approximated by the saturation temperature difference defined in Eq. (2).

2.5.5 Pressure-enthalpy diagram analysis

To enhance the accuracy of thermodynamic analysis, the pressure-enthalpy (P-h) diagram for water is used as a complementary analysis tool within the P-h framework. The P-h diagram provides a process-oriented representation of phase change phenomena and enables the visualization of evaporation and condensation in compact MED systems.

In the experimental configuration, the evaporation and condensation processes are conceptually mapped onto a P-h diagram. The evaporation process in the boiler and effect chamber occurs at the level of saturated liquid to saturated vapor. Conversely, the condensation process is an isenthalpic process, as shown in Figure 3.

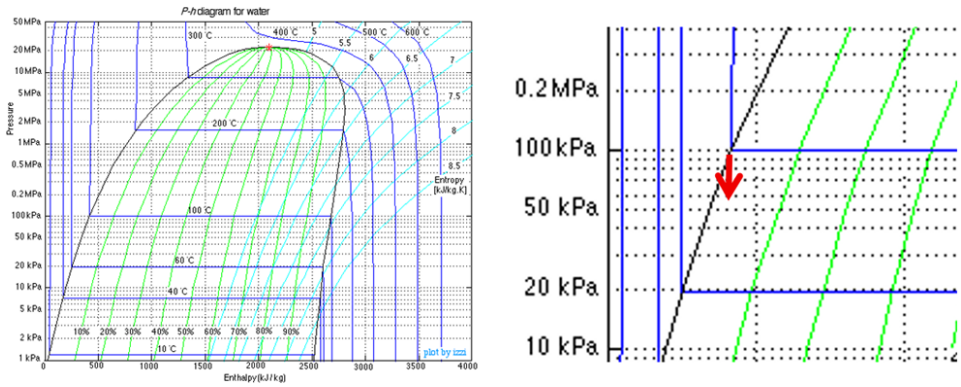

Figure 3. P-h diagram

3 Results

3.1 Experimental Setup

The experimental setup used in this study was a compact MED system, specifically designed to investigate the effect of pressure in freshwater tanks on freshwater production. This system integrates evaporation, condensation, and freshwater recovery components in a vertical and compact configuration.

This system consists of four main subsystems: the boiler room, two effect rooms, the condenser unit, and a closed fresh water recovery tank. The boiler room functions as the main heat input unit, where seawater is heated using gas until the desired operating pressure is reached. The steam produced flows sequentially through the first and second effect rooms, enabling the gradual utilisation of heat that is characteristic of MED systems. Each effect chamber is equipped with a spiral condenser made of 5/6-inch copper pipe.

One of the main features of the experimental setup is a sub-atmospheric pressure fresh water recovery tank. A vacuum pump is connected to this fresh water tank, allowing condensation pressure to be controlled without changing the evaporation pressure inside the boiler and effect chamber. This configuration establishes two separate pressure domains: the evaporation domain controlled by boiler pressure and the condensation domain controlled by freshwater tank pressure.

To ensure consistency between experiments, the system geometry, condenser configuration, volume of seawater supplied, and environmental conditions were kept constant. A supplied seawater volume of 500 mL was used for all trials, allowing direct comparison between freshwater results under different pressure combinations. Before the experiment began, the system was checked for leaks and allowed to reach stable operating conditions before data collection commenced. Figure 4 shows the configuration of the compact MED. Several main components consist of the first effect, second effect, coil heat exchanger, fresh water tube and dispenser frame.

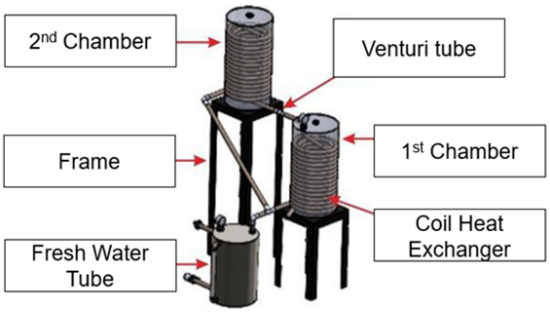

Figure 4. Design process

3.1.1 1st and 2nd chamber manufacture

The condenser tube design is intended to facilitate the manufacturing process of condenser tubes with dimensions planned according to the size of the tubes to be produced. The materials used in the manufacture of spiral condensers are copper pipes with a diameter of 5/16 inches and stainless-steel plates that have been shaped according to the diameter of the stainless-steel pipes (see Figure 5).

Figure 5. Chamber effect

3.1.2 Fresh water tube manufacture

The design of the fresh water tube is to facilitate the manufacturing process with the planning dimensions of the tube to be made with dimensions. The material used in the fresh water tube uses a 4-inch stainless steel pipe and a 101 mm diameter plate (see Figure 6).

Figure 6. Freshwater tank

3.2 Design of experiment

The experimental design was systematically designed to evaluate the impact of evaporation pressure and condensation pressure on fresh water production in a compact MED. A factorial experimental design was used in the testing process. Two operational parameters were set as independent variables: boiler pressure and fresh water recovery tank pressure. Boiler pressure indicates the evaporation conditions in the MED system, while fresh water tank pressure regulates the condensation boundary conditions. Each parameter was analysed at two different levels to evaluate their individual and collective impact on system performance.

The boiler pressure is set at 151.3 kPa and 201.3 kPa, indicating the low and high evaporation rates often observed in compact thermal desalination systems. The fresh water recovery tank pressure is set at 80 kPa and 70 kPa, corresponding to condensation conditions close to atmospheric pressure and below atmospheric pressure. The selected pressure levels are determined by the operational limitations of the experimental equipment to ensure stable and safe functioning. This combination of pressure levels results in four experimental configurations, labelled Experiment 1 to Experiment 4. Each configuration represents a unique pressure domain state, facilitating direct comparison of system performance across various combinations of evaporation-condensation pressures. The experimental design is listed in Table 1.

All variables were kept constant during testing. Constant variables included system geometry, condenser configuration, seawater supply volume, environmental conditions, and operational methods. A uniform seawater supply volume of 500 mL was used in all experiments to ensure consistency in freshwater production comparisons. Each experiment was conducted as a batch operation, and the system was allowed to reach stable operating conditions before data collection began. Pressure conditions were monitored continuously to ensure that target values were maintained during each run. The sequence of experiments was designed to minimise the effect of temperature transfer between consecutive tests. Figure 7 illustrates the experimental design used in the study.

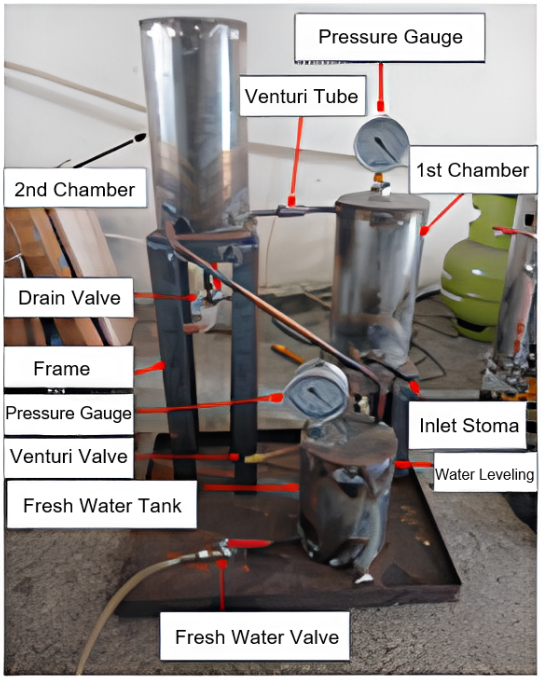

Figure 7. Testing components

The experimental steps were carried out in the following stages. Fill the boiler tube with seawater as needed, 500 mL. Attach a hose from the boiler to the copper pipe of the condenser tube. Connect a hose from the vacuum pump to the fresh water pipe and turn on the vacuum pump so that it shows negative pressure on the tube pressure gauge. Monitor the boiler pressure until it reaches the desired pressure by slightly opening the boiler steam valve. Record the fresh water results from the condenser tube every 1 minute and stabilise the pressure in the boiler and the sub-atmospheric pressure in the condenser tube.

3.3 Experimental Result

The cumulative fresh water production results obtained from Experiments 1–4 is presented in Figure 8 and Figure 9. The test results for boiler pressure of 151.3 kPa and fresh water pipe pressure of 80 kPa are shown in Figure 8a. The test was completed in 20 minutes with a fresh water production of 345 mL from a total of 500 mL of sea water.

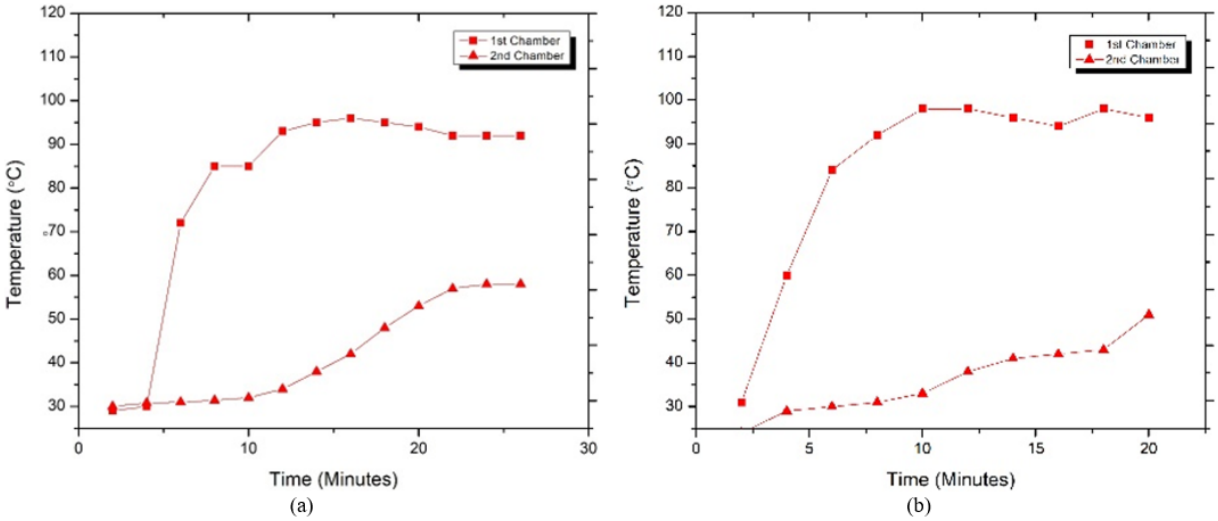

Figure 8. (a) Result of 1st experiment (151.3 kPa, 80 kPa); (b) Result of 2nd experiment 151.3 kPa, 70 kPa)

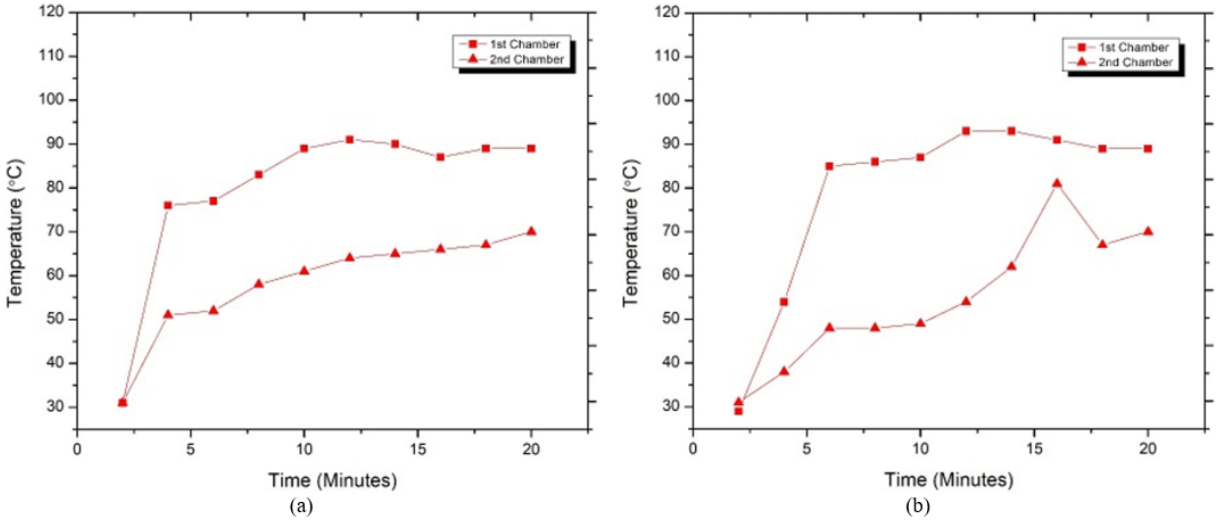

Figure 9. (a) Result of 3rd experiment (201.3 kPa, 80 kPa); (b) Result of 4th experiment 201.3 kPa, 70 kPa)

The freshwater production curve in 1st experiment shows a consistent and stable increase during the operational period. Total freshwater production reached 345 mL, indicating consistent condensation behaviour at pressures close to atmospheric pressure in the freshwater tank. In 2nd experiment, the freshwater tank pressure was changed to 70 kPa, resulting in a more pronounced cumulative freshwater production curve compared to Experiment 1. Overall freshwater production increased to 368.5 mL, indicating the highest production among all combinations evaluated.

The 3rd experiment was conducted at an elevated boiler pressure, while the freshwater tank pressure was maintained at 80 kPa. The freshwater production curve exhibits a heightened initial production rate, succeeded by

an earlier plateau. Notwithstanding the elevated evaporation pressure, the overall freshwater output was inferior to that achieved in 2nd experiment. In 4th experiment, the freshwater tank pressure was changed to 70 kPa while the boiler pressure was sustained at 201.3 kPa. The resultant production curve indicates enhanced freshwater generation relative to 3rd experiment. The overall output was inferior to that attained with moderate boiler pressure coupled with sub-atmospheric freshwater tank pressure.

The test results for boiler pressure 151.3 kPa and fresh water tube pressure 70 kPa. are shown in Figure 8b. The test was completed in 26 minutes with a fresh water yield of 368.5 mL from a total of 500 mL seawater. The test results for boiler pressure 201.3 kPa and fresh water tube pressure 80 kPa are shown in Figure 9a. The test was completed in 20 minutes with a fresh water yield of 310 mL from a total of 500 mL seawater. The test results for boiler pressure 201.3 kPa and fresh water tube pressure 70 kPa. are shown in Figure 9b. The test was completed in 20 minutes with a fresh water yield of 336 mL from a total of 500 mL seawater.

The results of testing the experimental variation of boiler pressure 151.3 kPa and 80 kPa fresh water tank pressure, in a test time of 20 minutes and filling the boiler tube using seawater 500 mL at the most fresh water yield at 8 minutes produced 170 mL with a total fresh water yield of 345 mL, experimental variation of boiler pressure 151.3 kPa and 70 kPa fresh water tank pressure, in a test time of 26 minutes and filling the boiler tube using seawater 500 mL at the most fresh water yield at 12 minutes produced 150 mL with a total fresh water yield of 368 mL, 5 mL, experiments with variations in boiler pressure of 1 bar and 80 kPa fresh water tank pressure, in a test time of 20 minutes and filling the boiler tube using seawater 500 mL at the most fresh water results in 10 minutes producing 160 mL with the total amount of fresh water results 310 mL, variations in boiler pressure of 1 bar and 80 kPa fresh water tank pressure in a test time of 20 minutes and filling the boiler tube using seawater 500 mL, at the most fresh water results in 6 minutes producing 120 mL with the total amount of fresh water results 336 ml. Such results can be shown in Table 2.

Table 2. Experimental results

No.	Boiler Pressure (kPa)	Freshwater Tank Pressure (kPa)	Result Volume (mL)			Average Volume (mL)
1	151.3	80	345	337	348	343.33
2	151.3	70	368.5	360	365	364.50
3	201.3	80	310	302	314	308.67
4	201.3	70	336	329	334.5	333.17

From the experimental data, a standard error value of 6.18 mL was obtained with an average experimental result of 337.42 mL, resulting in a relative error value of 1.83%. With these results, the average measurement accuracy is very good with an error value below 2%. From the observations made, the tendency of boiler pressure 151.3 kPa produces more fresh water production. For fresh water tube pressure, the lower the pressure the higher the fresh water produced. The results of the computational simulation in Aspen Hysys are shown in Table 3.

Table 3. Computational simulation result of Aspen Hysys

No.	Boiler Pressure (kPa)	Freshwater Tank Pressure (kPa)	Steam Boiler Mass Flow (kg/h)	Distillate Mass Flow (kg/h)	Total Brine (kg/h)
1	151.3	80	1	1.7067	1.2713
2	151.3	70	1	1.7188	1.2563
3	201.3	80	1	1.7140	1.2646
4	201.3	70	1	1.7255	1.2497

3.4 Thermodynamics Analysis

The thermodynamic conditions of the evaporation and condensation domains are determined using a saturated P-h diagram for water. In each experimental setup, the boiler pressure determines the saturation temperature associated with vapor formation, while the pressure of the fresh water recovery tank is at sub atmospheric pressure. A decrease in the pressure of the fresh water tank causes a decrease in the saturation condensation temperature, thereby increasing the effective temperature difference between the evaporation and condensation regions. This temperature difference serves as the main driving force for condensation heat transfer throughout the system (see Table 4).

The minimum heat requirement for condensation is calculated based on the freshwater production measured using the latent heat of vaporization. The calculated values for condensation heat load vary from approximately 534 W to 648 W under the operating conditions examined. Configurations with high condensation heat loads do not always align with increased freshwater production. This finding indicates that the effectiveness of condensation

and the efficiency of steam utilization are more significant than evaporation intensity alone in assessing the overall system performance. The effective UA of the condenser is evaluated to assess condensation performance. The fluctuation of UA in various experimental setups indicates the cumulative impact of heat transfer coefficient and effective condensation area under different pressure conditions. Sub-atmospheric freshwater tank pressure typically results in a more stable UA value, indicating more uniform condensation and improvement under sub-atmospheric conditions.

Table 4. Thermodynamics analysis

No.	Condensation Saturation Temp. (°C)	Condensation Driving Force (°C)	Condensation Heat Transfer (W)	Effective Heat Transfer Coefficient ($W \cdot K^{-1}$)
1	94.0	58.0	660	11.4
2	90.5	61.5	544	8.8
3	94.0	86.0	593	6.9
4	90.5	89.5	644	7.2

Table 5 presents a comparative reference between freshwater recovery ratios and gained output ratio (GOR) values. Single-stage VMD systems generally exhibit freshwater recovery ratios of 4–7% under high vacuum conditions due to their single-stage design [34]. An integrated MED system connected to an industrial waste heat source achieves a recovery ratio of approximately 35.85% [32], while a pilot-scale MED-AB system operates at a recovery ratio of 18–20% and a GOR value of 10–13 and a GOR value of 12–14 in a computational model [26]. Meanwhile, the current compact double-pressure MED system achieves a freshwater recovery ratio of up to 73.7% at sub-atmospheric condensation pressure (70–80 kPa) and a GOR value of 0.002–0.003.

Table 5. Benchmark comparison of multi-effect distillation (MED) performance

System Type	Configuration	Gained Output Ratio (GOR)	Freshwater Recovery Ratio (%)	Reference
Single stage vacuum-assisted membrane (VMD)	Vacuum membrane distillation	N/A	4–7	[34]
Large scale integrated MED	MED coupled with proton exchange membrane (PEM) electrolyser waste heat	N/A	35.85	[32]
MED–Absorber Compressor (MED-AB) pilot plant	MED-AB	10–13	18	[26]
MED-AB (virtual simulation platform simulation)	MED-AB (computational model)	12–14	20	[26]
Present type	Compact MED	0.002–0.003	73.7	This work

The thermodynamic patterns identified in this analysis correspond with the conceptual framework established by the P-h diagrams presented in the Methodology section. Specifically, sub-atmospheric assisted freshwater recovery alters the condensation process to a lower-pressure and lower-temperature environment, hence altering the thermodynamic pathway of vapor condensation without augmenting thermal input. This pressure-domain alteration improves the system's capacity to reclaim produced vapor as freshwater.

In the compact MED system analysed, steam generation in the boiler chamber and effects can be characterized as an evaporation process depicted on the P-h diagram with a path from the saturated liquid line to the saturated vapor line at the boiler pressure. Conversely, condensation in the freshwater recovery sector follows an almost isobaric heat rejection path from saturated vapor to the saturated liquid line at a reduced pressure level. Mapping the experimental conditions on a P-h diagram shows that the decrease in freshwater tank pressure shifts the condensation process to a lower pressure.

In experiment conducted at the same boiler pressure but varying freshwater tank pressures (trials 1 vs. 2 and Experiments 3 vs. 4), the P-h depiction demonstrates that the evaporation channel remains constant, however the condensation pathway is shifted downward on the figure. This verifies that the observed performance discrepancies stem predominantly from condensation-side thermodynamics, rather than alterations in evaporation intensity. The

increased distance between the evaporation and condensation trajectories on the P-h diagram under sub-atmospheric conditions correlates with the enhanced freshwater production and superior effective heat-transfer performance indicated in Table 2.

Additionally, the P-h diagram provides qualitative validation for the calculated effective UA values. Sub-atmospheric assisted condensation facilitates a more optimal transition from saturated vapor to saturated liquid, thereby minimizing the entropy generation associated with non-equilibrium condensation. This trend is evident in the more consistent UA values obtained at sub-atmospheric freshwater tank pressures, despite fluctuations in boiler pressure and condensation heat load.

4 Discussion

4.1 Condensation-Dominated Performance in Compact Multi-Effect Distillation Systems

The experimental and thermodynamic findings shown in Table 2 indicate that the freshwater production of the examined compact MED system is predominantly influenced by condensation-side thermodynamics, rather than only by evaporation intensity. While elevated boiler pressure enhances vapor generation capacity, the findings indicate that this augmentation does not inherently result in increased freshwater output unless condensation conditions are concurrently improved.

In all experimental setups, decreasing the pressure of the freshwater recovery tank reliably lowered the condensation saturation temperature (Eq. (1)), enhanced the condensation driving force (Eq. (2)), and boosted vapor utilization efficiency. This pattern indicates that pressure-domain adjustment on the condensation side is essential for improving freshwater recovery in compact thermal desalination systems.

The increase in freshwater yield noted under diminished freshwater tank pressure is mostly dictated by condensation-side thermodynamics rather than by evaporation-side heat input. Reducing the condensation pressure lowers the saturation temperature of water vapor, hence enhancing the effective temperature gradient between the vapor and the condenser surface. The Clausius-Clapeyron relation indicates that this pressure-induced shift enhances the condensation driving force and increases latent heat release rates, hence expediting the vapor-to-liquid phase transition.

Furthermore, sub-atmospheric operation inhibits the buildup of non-condensable gases in the condensation area. The diminished partial pressure of these gases alleviates gas blanketing effects and decreases interfacial thermal resistance, hence enhancing the effective condensation heat transfer coefficient. This mechanism elucidates the experimentally observed enhancement in the effective UA value with reduced freshwater tank pressures.

The pronounced sensitivity of freshwater yield to freshwater tank pressure underscores the pivotal significance of condensation-domain thermodynamics in compact MED systems. This pattern contrasts with traditional large-scale MED plants, where overall heat input predominantly dictates performance, suggesting that precise control of condensation-domain pressure is a crucial technique for enhancing performance in decentralized compact MED systems.

4.2 Interpretation Based on the Pressure-Enthalpy Diagram

The P-h diagram (Figure 3) of water elucidates the process-level rationale for the trends depicted in Table 2. For a specific boiler pressure, the evaporation trajectory on the P-h diagram is fundamentally consistent across studies. Conversely, decreasing the pressure of the freshwater tank alters the condensation pathway to a lower-pressure isobar, leading to a reduced condensation temperature and an altered entropy trajectory. The downward shift of the condensation path enhances the thermodynamic distinction between evaporation and condensation processes, directly correlating with the augmented condensation driving force (ΔT) computed using Eq. (2). On the P-h diagram, this is represented by an increased vertical temperature differential and a more advantageous latent heat rejection pathway, which promotes more thorough condensation of produced vapor. The T-s depiction elucidates why configurations with elevated boiler pressure but inadequate condensation driving power (e.g., Experiment 3) demonstrate increased initial vapor production while yielding lower cumulative freshwater output. In these instances, the condensation pathway remains next to the evaporation pathway on the T-s diagram, constraining efficient vapor recovery despite augmented heat input.

4.3 Relationship Between Condensation Heat Transfer and Heat Transfer Capacity

The computed condensation heat transfer rates (Eq. (3)) and effective heat transfer coefficients (UA, Eq. (4)) offer further understanding of condenser performance. Although elevated boiler pressure enhances the absolute heat transfer rate linked to condensation, the accompanying UA values do not increase correspondingly. This signifies that the effectiveness of heat transmission, rather than its magnitude, is the primary element influencing freshwater recovery. Sub-atmospheric condensation circumstances produce more consistent UA values across varying boiler pressures, indicating a more regulated and efficient condensation process. From a T-s standpoint, this aligns

with a condensation process that more accurately resembles an ideal saturated-vapor-to-saturated-liquid transition, exhibiting diminished non-equilibrium effects and reduced entropy formation during the phase change.

4.4 Generalizability and Scalability of the Proposed Dual-Pressure Multi-Effect Distillation Approach

The current work utilized a small two-effect MED prototype; however, the suggested dual-pressure-domain condensation technique is not intrinsically confined to the evaluated geometry or scale. The primary mechanism regulating performance improvement—specifically, the targeted decrease of condensation-domain pressure to amplify the condensation driving force and reduce non-condensable gas buildup—is independent of scale and based on saturation thermodynamics and interfacial heat transfer dynamics.

The thermodynamic-computational framework utilized in this study, which incorporates saturation temperature shifting, condensation driving-force assessment, and effective UA characterization, can be readily adapted to multi-effect MED systems with increased numbers of effects by applying the same lumped-parameter modelling to each condensation stage. Moreover, modular MED devices can emulate the suggested sub-atmospheric assisted freshwater recovery tank as a standalone condensation domain, facilitating decentralized or mobile desalination applications without augmenting thermal input on the evaporation side.

The technique is scalable and compatible with both waste-heat-driven and renewable-assisted MED designs. As system size expands, the condensation-domain pressure manipulation technique continues to be relevant, providing a means for performance enhancement via precise vacuum regulation instead of augmented heating capacity, thereby maintaining energy economy in larger implementations.

5 Conclusions

This study experimentally evaluated the effectiveness of a compact MED system at various combinations of boiler pressure and fresh water tank pressure. Experimental observations show that a decrease in fresh water tank pressure from 80 kPa to 70 kPa causes an increase in the volume of fresh water collected from 345 mL to 368.5 mL at a boiler pressure of 151.3 kPa. Computational simulations using Aspen Hysys show that the total distillate mass flow is highest at a pressure of 70 kPa.

Thermodynamic research using the Clausius-Clapeyron approach shows that sub-atmospheric pressure in the fresh water tank reduces the saturation condensation temperature from approximately 94℃ to 90.5℃. This decrease increases the calculated condensation driving force (ΔT) for all experimental settings operating at lower fresh water tank pressures. The calculated condensation heat transfer rate and effective UA indicate that increased fresh water production is more closely related to ideal condensation conditions than simply increasing boiler pressure.

Analysis of the P-h diagram for water shows that fresh water production results from changes in the condensation path in the water fraction, while the evaporation path remains stable at the specified boiler pressure. A decrease in condensation pressure shifts the condensation process to a lower temperature range, thereby increasing steam condensation efficiency. These findings indicate that fresh water tank pressure is a crucial variable in the compact MED system analysed, and that fresh water recovery with the aid of sub-atmospheric pressure increases fresh water yield by modifying the thermodynamics of condensation within the operational parameters studied.

Author Contributions

Conceptualization, E.K.; methodology, E.K. and U.G.S.D.; formal analysis, E.K.; investigation, E.K. and D.P.; data curation, H.S.; writing—original draft preparation, E.K.; writing—review and editing, E.K.; visualization, S.R.; supervision, U.G.S.D.; project administration, U.G.S.D and H.S. All authors were actively involved in discussing the findings and refining the final manuscript.

Funding

This work is funded by Kemdikbud Ristek (Grant No.: 125/C3/DT.05.00/PL/2025); Lldikti IV (Grant No.: 8032/LL4/PG/2025); Universitas Majalengka (Grant No.: 142/KL/LP2MI UNMA/2025).

Data Availability

The data used to support the findings of this study are available from the corresponding author upon request.

Conflicts of Interest

The authors declare no conflict of interest.

References

[1] R. Smith, *Chemical Process: Design and Integration*. John Wiley & Sons, 2005.

[2] A. A. Kiss, "Distillation technology—Still young and full of breakthrough opportunities," *J. Chem. Technol. Biotechnol.*, vol. 89, no. 4, pp. 479–498, 2014. https://doi.org/10.1002/jctb.4262

[3] Ž. Olujić, L. Sun, A. de Rijke, and P. J. Jansens, "Conceptual design of an internally heat integrated propylene-propane splitter," *Energy*, vol. 31, no. 15, pp. 3083–3096, 2006. https://doi.org/10.1016/j.energy.2006.03.030

[4] I. J. Halvorsen and S. Skogestad, "Liquid-only transfer in dividing wall columns—Analytical minimum vapor expressions," *Sep. Purif. Technol.*, vol. 365, p. 132530, 2025. https://doi.org/10.1016/j.seppur.2025.132530

[5] A. S. Nafey, H. E. S. Fath, and A. A. Mabrouk, "Thermoeconomic design of a multi-effect evaporation mechanical vapor compression (MEE-MVC) desalination process," *Desalination*, vol. 230, no. 1-3, pp. 1–15, 2008. https://doi.org/10.1016/j.desal.2007.08.021

[6] U. Dinata, J. Kurniawan, and A. Havendry, "Experimental analysis of flash evaporation desalination with solar energy," in *Proceeding of 5th Indonesian Student's Scientific Meeting*, Paris, France, 2000, pp. 171–174.

[7] J. Koschikowski, M. Wieghaus, and M. Rommel, "Solar thermal-driven desalination plants based on membrane distillation," *Desalination*, vol. 156, no. 1-3, pp. 295–304, 2003. https://doi.org/10.1016/S0011-9164(03)00360-6

[8] E. Koswara, Nasim, and F. Rahmanudin, "Analysis of the effect of distillation parameters on freshwater yield in seawater dispenser," in *Proceeding of 3rd International Symposium on Advances and Innovation in Mechanical Engineering (ISAIME 2022)*, Makassar, Indonesia, 2022, p. 012002. https://doi.org/10.1088/1742-6596/2739/1/012002

[9] E. Koswara, H. Sonawan, and N. N. Suryaman, "Improving freshwater yield from simple seawater distillation dispensers through condenser pipe modifications," *ASEAN Eng. J.*, vol. 14, no. 3, pp. 191–196, 2024. https://doi.org/10.11113/aej.v14.21654

[10] E. Koswara, D. Susandi, H. Sujadi, H. Sonawan, T. Setiawan, U. Komarudin, and A. Siswanto, "Design and control of boiler systems for enhanced performance in mini-MED applications," *Int. J. Heat Technol.*, vol. 43, no. 1, pp. 353–360, 2025. https://doi.org/10.18280/ijht.430136

[11] E. Koswara, H. Sonawan, H. Sujadi, E. D. Jannati, D. Ariandoyo, and F. Rahmanudin, "Development of a sea water dispenser automation system to improve distillation process efficiency," in *Proceedings of the International Conference on Science Technology and Social Sciences—Physics, Material and Industrial Technology (ICONSTAS-PMIT 2023)*, Shah Alam, Malaysia, 2024, pp. 41–51. https://doi.org/10.2991/978-94-6463-500-3_5

[12] E. Cardona and A. Piacentino, "Optimal design of cogeneration plants for seawater desalination," *Desalination*, vol. 166, pp. 411–426, 2004. https://doi.org/10.1016/j.desal.2004.06.096

[13] M. Alhaj, A. Hassan, M. Darwish, and S. G. Al-Ghamdi, "A techno-economic review of solar-driven multi-effect distillation," *Desalin. Water Treat.*, vol. 90, pp. 86–98, 2017. https://doi.org/10.5004/dwt.2017.21297

[14] G. Zaragoza, J. A. Andrés-Mañas, and A. Ruiz-Aguirre, "Commercial scale membrane distillation for solar desalination," *NPJ Clean Water*, vol. 1, p. 20, 2018. https://doi.org/10.1038/s41545-018-0020-z

[15] S. A. Kalogirou, *Solar Energy Engineering: Processes and Systems*. Elsevier, 2023.

[16] Z. M. Omara, A. E. Kabeel, and M. M. Younes, "Enhancing the stepped solar still performance using internal and external reflectors," *Energy Convers. Manag.*, vol. 78, pp. 876–881, 2014. https://doi.org/10.1016/j.enconman.2013.07.092

[17] H. N. Panchal and S. Patel, "An extensive review on different design and climatic parameters to increase distillate output of solar still," *Renew. Sustain. Energy Rev.*, vol. 69, pp. 750–758, 2017. https://doi.org/10.1016/j.rser.2016.09.001

[18] A. S. Jawed, L. Nassar, H. M. Hegab, R. van der Merwe, F. Al Marzooqi, F. Banat, and S. W. Hasan, "Recent developments in solar-powered membrane distillation for sustainable desalination," *Heliyon*, vol. 10, no. 11, p. e31656, 2024. https://doi.org/10.1016/j.heliyon.2024.e31656

[19] G. N. Tiwari and L. Sahota, "Review on the energy and economic efficiencies of passive and active solar distillation systems," *Desalination*, vol. 401, pp. 151–179, 2017. https://doi.org/10.1016/j.desal.2016.08.023

[20] S. Kalogirou, "Seawater desalination using renewable energy sources," *Prog. Energy Combust. Sci.*, vol. 31, no. 3, pp. 242–281, 2005. https://doi.org/10.1016/j.pecs.2005.03.001

[21] Z. M. Omara, A. E. Kabeel, and A. S. Abdullah, "A review of solar still performance with reflectors," *Renew. Sustain. Energy Rev.*, vol. 68, pp. 638–649, 2017. https://doi.org/10.1016/j.rser.2016.10.031

[22] A. Alkaisi, R. Mossad, and A. Sharifian-Barforoush, "A review of the water desalination systems integrated with renewable energy," *Energy Procedia*, vol. 110, pp. 268–274, 2017. https://doi.org/10.1016/j.egypro.2017.03.138

[23] H. T. El-Dessouky and H. M. Ettouney, *Fundamentals of Salt Water Desalination*. Elsevier, 2002.

[24] S. Zhou, L. Gong, X. Liu, and S. Shen, "Mathematical modeling and performance analysis for multi-effect evaporation/multi-effect evaporation with thermal vapor compression desalination system," *Appl. Therm. Eng.*, vol. 159, p. 113759, 2019. https://doi.org/10.1016/j.applthermaleng.2019.113759

[25] C. A. C. D. la Torre, N. Velázquez-Limón, R. López-Zavala, J. Ríos-Arriola, S. Islas-Pereda, G. E. Dévora-Isiordia, and J. A. Aguilar-Jiménez, "High vacuum multiple effect desalination system with barometric ejector condensation," *Desalination*, vol. 586, p. 117842, 2024. https://doi.org/10.1016/j.desal.2024.117842

[26] S. Aly, J. Jawad, H. Manzoor, S. Simson, J. Lawler, and A. N. Mabrouk, "Pilot testing of a novel integrated multi effect distillation-Absorber Compressor (MED-AB) technology for high performance seawater desalination," *Desalination*, vol. 521, p. 115388, 2022. https://doi.org/10.1016/j.desal.2021.115388

[27] Z. Dai, B. Li, and S. Elbel, "Advances in ejector research for multi-effect thermal vapor compression desalination," *Renew. Sustain. Energy Rev.*, vol. 208, p. 115010, 2025. https://doi.org/10.1016/j.rser.2024.115010

[28] M. Sheta and H. Hassan, "Investigation of multi-effect mechanical vapor compression desalination system powered by photovoltaic/thermal, photovoltaic-evacuated tubes, and photovoltaic solar collectors: Techno-economic study," *Appl. Therm. Eng.*, vol. 236, p. 121584, 2024. https://doi.org/10.1016/j.applthermaleng.2023.121584

[29] M. A. Kotb and A. E. Khalifa, "A novel vacuum membrane distillation system with water ejector: Performance assessment and optimization," *Energy Convers. Manag.*, vol. 343, p. 120239, 2025. https://doi.org/10.1016/j.enconman.2025.120239

[30] S. A. Romo, M. Storch, Jr., and J. Srebric, "Operation modeling and comparison of actual multi-effect distillation and reverse osmosis desalination plants," *Desalination*, vol. 571, p. 117046, 2024. https://doi.org/10.1016/j.desal.2023.117046

[31] B. Shahzamanian, S. Varga, J. Soares, A. I. Palmero-Marrero, and A. C. Oliveira, "Theoretical performance assessment of a multi-effect distillation system integrated with thermal vapour compression unit running on solar energy," *Int. J. Low-Carbon Technol.*, vol. 19, pp. 908–921, 2024. https://doi.org/10.1093/ijlct/ctae010

[32] M. Haqiqi, S. Dussi, and J. Garcia-Navarro, "Multi-effect distillation for water desalination in an offshore PEM electrolyser system," *Energy Rep.*, vol. 14, pp. 1452–1466, 2025. https://doi.org/10.1016/j.egyr.2025.07.031

[33] O. Shamet and M. Antar, "Mechanical vapor compression desalination technology—A review," *Renew. Sustain. Energy Rev.*, vol. 187, p. 113757, 2023. https://doi.org/10.1016/j.rser.2023.113757

[34] W. Bibi, M. Asif, F. Iqbal, and J. Rabbi, "Hybrid vacuum membrane distillation-multi effect distillation (VMD-MED) system for reducing specific energy consumption in desalination," *Desalin. Water Treat.*, vol. 317, p. 100064, 2024. https://doi.org/10.1016/j.dwt.2024.100064